ISSN 1607-0763 (Print); ISSN 2408-9516 (Online)
https://doi.org/10.24835/1607-0763-1247

Texture and CT-features in differentiation of hypervascular pancreatic neuroendocrine tumors from renal cell carcinoma metastases: diagnostic model

© **Ivan S. Gruzdev[1]*, Grigory G. Karmazanovsky[1], Mariya G. Lapteva[2], Kseniia A. Zamiatina[1], Valeriya S. Tikhonova[1], Evgeny V. Kondratyev[1], Vladimir Yu. Struchkov[1], Andrey V. Glotov[1], Ilya S. Proskuryakov[2], Danil V. Podluzhnyi[2], Amiran Sh. Revishvili[1]**

[1] A.V. Vishnevsky National Medical Research Center of Surgery of the Ministry of Healthcare of the Russian Federation; 27, Bol'shaya Serpukhovskaia str., Moscow, 117997, Russian Federation

[2] N.N. Blokhin National Medical Research Center of Oncology of the Ministry of Healthcare of the Russian Federation; 23, Kashirskoe shosse, Moscow, 115478, Russian Federation

Objective: to develop a diagnostic model that includes CT and radiomic features for the differential diagnosis of pancreatic neuroendocrine tumors (PNETs) G1 and G2 and pancreatic renal cell carcinoma (RCC) metastases.

Material and Methods. 78 patients with 79 hypervascular PNETs and 17 patients with 24 pancreatic RCC metastases who underwent pancreatic resection and histological verification were selected in the study. All the patients underwent preoperative contrast enhanced CT (CECT). We assessed tumor attenuation, composition (cystic/solid), homogeneity (homogeneous/heterogeneous), calcification and presence of the main pancreatic duct (MPD) dilation. We calculated lesion-to-parenchyma contrast (LPC), relative tumor enhancement ratio (RTE) and extracted 52 texture features for arterial phase of CECT. Qualitative and texture features were compared between PNETs and pancreatic RCC metastasis. The selection of predictors for the logistic model was carried out in 2 successive stages: 1) selection of predictors based on one-factor logistic models, the selection criterion was $p < 0.2$; 2) selection of predictors using L2 regularization (LASSO regression after standardization of independent variables). The selected predictors were included in a logistic regression model without interactions, the coefficients of which were estimated using the maximum likelihood method with a penalty of 0.8.

Results. There was no difference in composition, homogeneity (homogeneous/heterogeneous) and presence of the MPD dilation between groups. We did not find calcification in pancreatic RCC metastasis, in contrast to the PNETs (9% contained calcifications). After selection, the LCR, CONVENTIONAL_HUmin, GLCM_Correlation, NGLDM_Coarseness were included in the final diagnostic model, which showed a sensitivity and specificity of 95.8%; 62% in the prediction of pancreatic RCC metastases.

Conclusion. The diagnostic model developed on the basis of texture and CT-features has high sensitivity (95.8%) with moderate specificity (62%), which allows it to be used in complex diagnostic cases to determine the patient's treatment tactics.

Keywords: computed tomography, texture analysis, renal cell carcinoma, metastases, pancreatic neuroendocrine tumor

Conflict of interest. Acknowledgments: The reported study was funded by RFBR, project number 20-315-90070.

For citation: Gruzdev I.S., Karmazanovsky G.G., Lapteva M.G., Zamyatina K.A., Tikhonova V.S., Kondratyev E.V., Struchkov V.Yu., Glotov A.V., Proskuryakov I.S., Podluzhny D.V., Revishvili A.Sh. Texture and CT-features in differentiation of hypervascular pancreatic neuroendocrine tumors from renal cell carcinoma metastases: diagnostic model. *Medical Visualization.* 2022. https://doi.org/10.24835/1607-0763-1247

Received: 29.07.2022. **Accepted for publication:** 16.09.2022. **Published online:** 1.11.2022.

Текстурные и КТ-признаки в дифференциальном диагнозе гиперваскулярных нейроэндокринных опухолей поджелудочной железы и метастазов почечно-клеточного рака: диагностическая модель

© **Груздев И.С.[1]*, Кармазановский Г.Г.[1], Лаптева М.Г.[2], Замятина К.А.[1], Тихонова В.С.[1], Кондратьев Е.В.[1], Стручков В.Ю.[1], Глотов А.В.[1], Проскуряков И.С.[2], Подлужный Д.В.[2], Ревишвили А.Ш.[1]**

[1] ФГБУ "Национальный медицинский исследовательский центр хирургии им. А.В. Вишневского" Минздрава России; 117997 Москва, ул. Большая Серпуховская, д. 27, Российская Федерация

[2] ФГБУ "Национальный медицинский исследовательский центр онкологии им. Н.Н. Блохина" Минздрава России; 115478, Москва, Каширское шоссе, д. 23, Российская Федерация

Цель исследования: разработать диагностическую модель, включающую КТ-характеристики и показатели радиомики для дифференциальной диагностики нейроэндокринных опухолей поджелудочной железы (ПНЭО) G1 и G2 и метастазов почечно-клеточного рака (ПКР).

Материал и методы. В исследование были отобраны 78 пациентов с 79 гиперваскулярными ПНЭО и 17 пациентов с 24 метастазами ПКР, которым была выполнена резекция поджелудочной железы с гистологической верификацией. Всем пациентам перед операцией была проведена КТ с контрастным усилением. Мы оценивали плотность опухоли, структуру (кистозная/солидная), гомогенность (гомогенная/гетерогенная), кальцификацию и наличие расширения главного протока поджелудочной железы (ГПП). Мы рассчитали отношение плотности опухоли к плотности паренхимы (LPC) и относительный коэффициент контрастирования опухоли (RTE) и вычислили 52 текстурных показателя для артериальной фазы КТ-исследования. Качественные и текстурные характеристики сравнивали между ПНЭО и метастазами ПКР. Отбор предикторов в логистическую модели осуществлялся в 2 последовательных этапа: 1) отбор предикторов на основе однофакторных логистических моделей, критерием отбора служило $p < 0.2$; 2) отбор предикторов с помощью L2-регуляризации (LASSO-регрессия после стандартизации независимых переменных). Отобранные предикторы включались в логистическую регрессионную модель без взаимодействий, коэффициенты которой рассчитывались с использованием метода максимального правдоподобия со штрафом 0,8.

Результаты. Не было различий в структуре, гомогенности (гомогенные/гетерогенные) и наличии дилатации ГПП между группами. Мы не обнаружили кальцификации при метастазах ПКР, в отличие от ПНЭО. После отбора LCR, CONVENTIONAL_HUmin, GLCM_Correlation, NGLDM_Coarseness были включены в окончательную диагностическую модель, которая показала чувствительность и специфичность 95.8%; 62% в прогнозировании метастазов ПКР.

Заключение. Разработанная на основании текстурных и КТ-признаков диагностическая модель обладает высокой чувствительностью (95.8%) при умеренной специфичности (62%), что позволяет использовать ее при сложных диагностических случаях для определения тактики лечения пациента.

Ключевые слова: компьютерная томография, текстурный анализ, почечно-клеточный рак, метастазы, нейроэндокринная опухоль поджелудочной железы

Источники финансирования и конфликт интересов. Источники финансирования: Исследование выполнено при финансовой поддержке РФФИ в рамках научного проекта № 20-315-90070.

Для цитирования: Груздев И.С., Кармазановский Г.Г., Лаптева М.Г., Замятина К.А., Тихонова В.С., Кондратьев Е.В., Стручков В.Ю., Глотов А.В., Проскуряков И.С., Подлужный Д.В., Ревишвили А.Ш. Текстурные и КТ-признаки в дифференциальном диагнозе гиперваскулярных нейроэндокринных опухолей поджелудочной железы и метастазов почечно-клеточного рака: диагностическая модель. *Медицинская визуализация.* 2022. https://doi.org/10.24835/1607-0763-1247

Поступила в редакцию: 29.07.2022. **Принята к печати:** 16.09.2022. **Опубликована online:** 1.11.2022.

Introduction

Renal cell carcinoma (RCC) annually causes the death of 30,000 patients in Europe [1, 2]. At the same time, RCC is the most common malignant tumor that metastasizes to the pancreas. The method of choice for diagnosing both kidney cancer and pancreatic tumors is contrast enhanced computed tomography [3, 4]. The most common pancreatic tumor is hypovascular intraductal adenocarcinoma, which, according to CT-features, significantly differs from renal cell carcinoma and its metastases [5]. At the same time, rather rare pancreatic neuroendocrine tumors (PNETs) grade 1 (G1) and grade 2 (G2) have similar contrast enhancement characteristics with pancreatic RCC metastases, being hypervascular compared to the intact pancreatic parenchyma [6]. Additional difficulties are caused by clinical situations when pancreatic RCC metastasis to the pancreas is the only manifestation of the disease after a long time after surgical treatment of kidney cancer [7, 8].

The management of PNETs and pancreatic RCC metastases differs. The only radical treatment for PNETs is surgical resection [9, 10]. However, for small, non-functioning tumors the radiological follow up or immunotherapy could be considered [11]. Patients with RCC metastases are recommended to undergo pancreatic resection or targeted immunotherapy [12, 13]. Accurate preoperative differential diagnosis allows early treatment and avoids additional invasive interventions such as fine needle biopsy.

Recently, radiomic features have shown promising results in the differential diagnosis of various pancreatic tumors [14–16]. van der Pol et al. compared the quantitative and qualitative CT characteristics of 43 resected PNETs and 28 pancreatic RCC metastases and found that the radiomic feature entropy has moderate sensitivity and specificity (71.4/79.1%, respectively) in the diagnosis of PNETs [17].

The purpose of our study was to develop a diagnostic model based on CT and radiomic features for the differential diagnosis of PNETs G1 and G2 and pancreatic RCC metastases.

Material and Methods

This retrospective study, based on patient data from A. V. Vishnevsky National Medical Research Center of Surgery and N. N. Blokhin National Medical Research Center of Oncology, was approved by the decision of the local ethics committee, Protocol No. 008-2019 dated September 27, 2019.

Study population

The study included 78 patients with PNETs G1 and G2 and 17 patients with RCC metastases to the pancreas. All patients underwent preoperative CECT. The inclusion criterion was the presence of the unenhanced and arterial phases of the CT examination. The inclusion criterion for patients with PNETs was the availability of data from an immunohistochemical study with grade determination. All patients with pancreatic RCC metastases underwent surgery and subsequent morphological verification.

Morphology and immunohistochemistry

Analyzes of the gross specimens were performed in the pathoanatomical departments of the A.V. Vishnevsky National Medical Research Center of Surgery and N.N. Blokhin National Medical Research Center of Oncology. PNETs were graded according to the guidelines of the World Health Organization (WHO, 2020) based on the mitotic count and the Ki-67 index. The grade was determined based on the value of the Ki-67 proliferation index and mitotic count in 10 fields of view (G1 – Ki-67 $\leqslant$ 2, mitotic count <2, G2 – Ki-67 = 2–20, mitotic count = 2–20).

CT acquisition

The majority of patients (50 patients with PNETs and 1 patient with RCC metastasis to pancreas) underwent CECT according to the standard protocol of the N.N. A. V. Vishnevsky. The following scanning parameters were used: slice thickness 1.5 mm, tube voltage 100 kV, reconstruction gap 0.75 mm. A contrast agent with an iodine concentration of 350 mg/ml was injected using an automatic injector at a rate of 3.5 ml/s, followed by the injection of 25 ml of saline. The volume of the contrast agent was calculated according to the formula 1 ml/kg of the patient's body weight, but not more than 100 ml. Contrast enhanced imaging was performed using the "bolus traking" technique with a density threshold of 150 HU on the descending thoracic aorta at the level of the diaphragm, starting the arterial phase scan for 10 s. CT scans of the rest of the patients (44) were performed on different CT-machines. The slice thickness varied from 1 to 5 mm, and the tube voltage varied from 100 to 140 kV. The inclusion criteria were the presence of the native and arterial phases of the CECT.

Qualitative CT analysis

Two radiologists with 3 and 12 years of abdominal imaging experience measured the density of tumor tissue and intact pancreatic parenchyma. In tumors, the most contrast-enhancing component of the tumor was measured by the largest possible region of interest. In the case of a heterogeneous tumor structure, areas of cystic degeneration of the tumor and the zones of calcifications were avoided. In the pancreatic parenchyma, the most representative area was measured with no calcifications, cystic inclu-

sions, and atrophy. In pancreatic RCC metastases, well-demarcated lesions whose maximum size exceeded twice the section thickness (2–10 mm) were selected for analysis. Next, we calculated the ratio of PNET density to the density of intact pancreatic tissue LPC (Lesion to Parenchyma) and the relative tumor enhancement ratio (RTE) for the arterial phase of the study using the following formulas:

$$LPC = Ta/Pa,$$
$$RTE = (Ta - Tn)/(Pa - Pn)$$

Ta – the density of the tumor tissue in the arterial phase, Pa – the density of the parenchyma in the arterial phase, Tn – the density of the tumor tissue in the unenhanced phase, Pn – the density of the parenchyma in the unenhanced phase.

The presence and absence of the following CT features were assessed in pancreatic tumors: cysts, calcifications, homogeneity, main pancreatic duct dilatation, pancreatic parenchymal atrophy.

Radiomic analysis

The open-source software the LIFEx application (version v5.10, www.lifexsoft.org) was used to calculate texture features [18]. Segmentation of the entire tumor volume was performed using a three-dimensional region of interest (3D ROI) in the arterial phase of the study (Fig. 1). After segmentation, 52 radiomic features were automatically calculated for arterial phase of the study. Textural features were selected from them, in which the Kendall concordance coefficient was 0.7 or more [19].

Statistical analysis

Data analysis was carried out using the R 4.1.0 statistical computing environment (R Foundation for Statistical Computing, Vienna, Austria).

To analyze the consistency of qualitative scores between two radiologists, type I intraclass correlation coefficient (ICC) was used for quantitative variables and Cohen's kappa statistic (κ) for binary variables.

The selection of predictors for the logistic model was carried out in 2 successive stages: 1) selection of predictors based on one-factor logistic models, the selection criterion was $p < 0.2$; 2) selection of predictors using L2 regularization (LASSO regression after standardization of independent variables, hyperparameter λ was determined using 10-box cross-validation while minimizing model deviation). The selected predictors were included in a logistic regression model without interactions, the coefficients of which were estimated using the maximum likelihood method with a penalty of 0.8 (Penalised maximum likelihood estimator). Model characteristics were evaluated using a nonparametric bootstrap (B = 100).

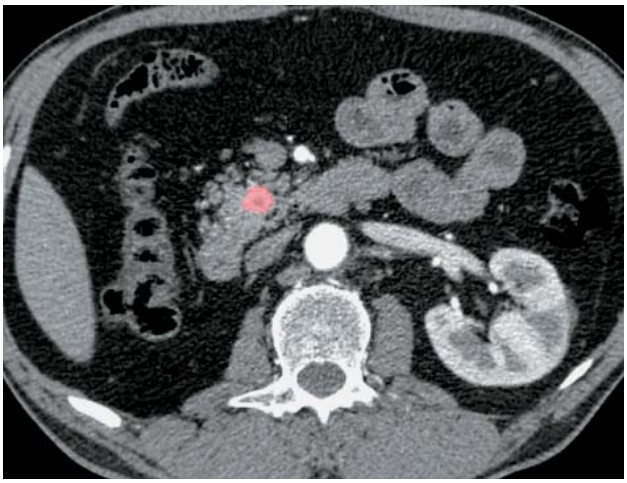

Fig. 1. CECT in a patient with RCC metastasis in the head of the pancreas, arterial phase. The entire visible volume of the metastases is segmented.

Results

A total of 79 resected PNETs in 78 patients and 24 pancreatic RCC metastases in 17 patients were included in the study. Among patients with PNETs, 25 patients underwent tumor enucleation, 12 pancreatoduodenal resection, 8 median pancreatic resection, 32 distal pancreatic resection, and 1 total pancreatectomy.

Table present the results of an analysis of the agreement between the scores of two radiologists regarding contrast ratios. It was found that, in general, the consistency of the scores was satisfactory, however, as can be seen from Table 1, the consistency depended on the diagnosis and was significantly higher when evaluating the contrast features in the case of PNETs. In general, LCR is more consistent

Table. Consistency of Radiologists' Assessments. ICC – intraclass correlation coefficient, CI – confidence interval

Index	PNETs + RCC metastases		PNETs		RCC metastases	
	ICC [95% CI]	P	ICC [95% CI]	P	ICC [95% CI]	P
LCR	0.62 [0.49; 0.73]	<0.0001	0.73 [0.60; 0.82]	<0.0001	0.18 [–0.18; 0.51]	0.1663
RTE	0.58 [0.43; 0.69]	<0.0001	0.68 [0.53; 0.79]	<0.0001	0.23 [–0.12; 0.56]	0.0996

than RTE, which can be explained by a simpler formula for its calculation and fewer measurements.

Among CT features, all criteria were in full agreement, except for the presence of calcifications, since no calcifications were detected in the structure of RCC metastases to pancreas, and homogeneity of contrast enhancement. In our opinion, the assessment of contrast homogeneity is too subjective, as it may vary with changes in image contrast, which may affect the results of the differential diagnosis.

After applying single-factor logistic models, 13 texture features were selected for further selection of predictors in a multi-factor model. There was a strong correlation between LCR and RTE scores (ρ = 0.93 [95% CI: 0.9–0.95]), with no significant difference in association with diagnosis in univariate models (AUC = 0.76 vs. AUC = 0.77 for LCR and RTE respectively). So it was decided to include the LCR in the subsequent selection due to a slightly higher consistency of assessments by radiologists (Table).

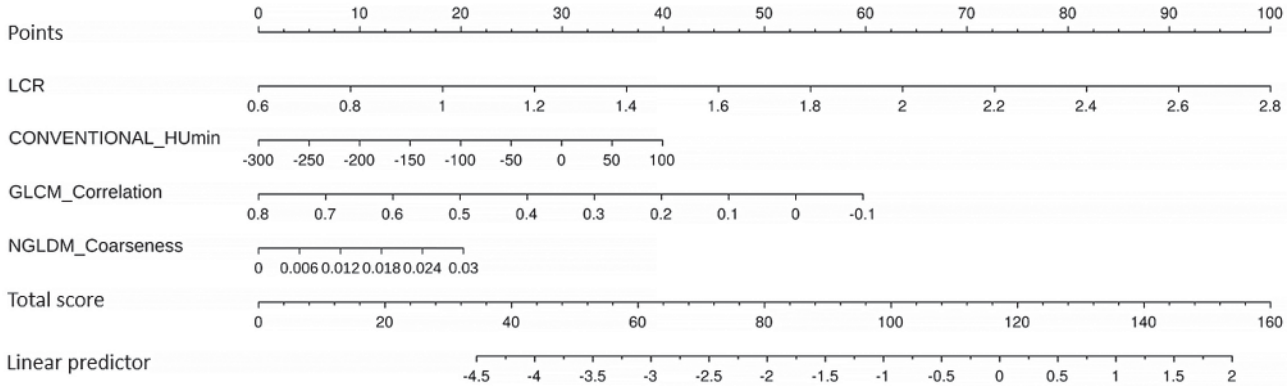

Fig. 2. Nomogram for assessing the probability of pancreatic RCC metastasis. To assess the value of the logistic function (a linear combination of predictors) and the probability of an outcome, it is necessary to determine the corresponding score for each predictor, then sum the scores for all predictors. Using the corresponding score and the diagram (Fig. 3), the probability of presence a RCC metastasis is calculated.

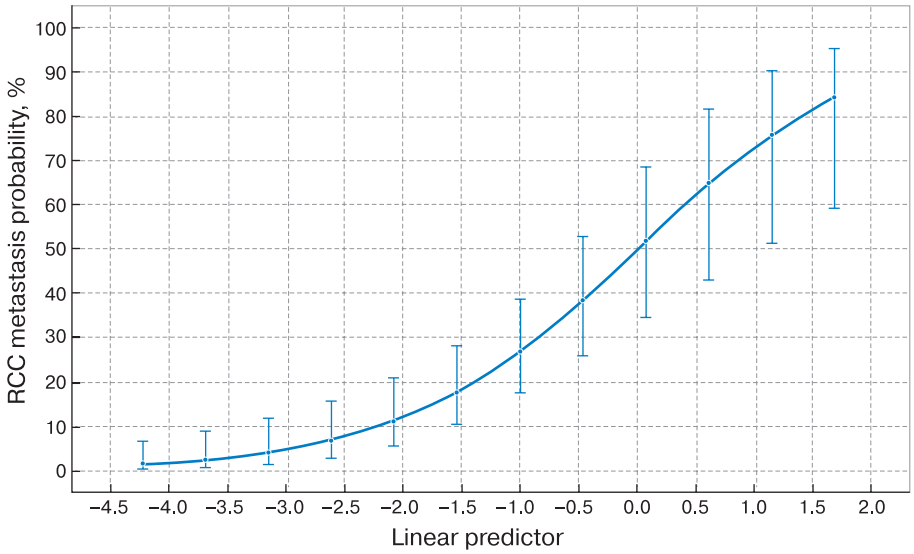

Fig. 3. Estimation of the accuracy of predictions obtained in the multiple logistic regression model. The points correspond to the estimates of the probability RCC metastasis depending on the values of the linear predictor, the vertical lines correspond to the standard errors of predictions. For example, the final score = 1,7 (from Fig. 2) corresponds to the probability of a RCC metastasis 85%.

When using L2 regularization, 4 predictors, 1 contrast ratio (LCR) and 3 texture features were selected in the final model:

• CONVENTIONAL_HUmin – characterizes the minimum voxel value (HU) in the region of interest

• GLCM_Correlation (Grey Level Co-occurrence Matrix Correlation) – Correlation in the gray level coincidence matrix, linear dependence of gray levels in GLCM

• NGLDM_Coarseness (Neighborhood Grey-Level Difference Matrix Coarseness), gray neighborhood difference matrix. NGLDM characterizes the difference in gray level between a voxel and its 26 neighboring voxels in three spatial dimensions. NGLDM_Coarseness is the spatial rate of change in gray level intensity.

Figures 2–3 present a nomogram for the probability of pancreatic RCC metastases derived from the final model. The resulting model was characterized by the following characteristics: Nigelkerke's pseudo-R2 was 0.35 (Nijelkirk's adjusted pseudo-R2 was 0.31) and C-index (AUC) was 0.82 [95% CI: 0.74; 0.91] (adjusted C-index – 0.79). The developed diagnostic model had a sensitivity and specificity of 95.8%; 62%, respectively, in the diagnosis of RCC metastases to pancreas (Youden index = 16%).

Discussion

The number of publications devoted to the differential diagnosis of PNETs and pancreatic RCC metastases is extremely small, since metastases are a fairly rare pathology of the pancreas compared to pancreatitis and primary tumors. Moreover, a very small proportion of patients undergo surgical treatment due to limited indications. At the same time, large medical centers with a large volume of surgical interventions in the hepatobiliary zone accumulate a fairly large number of patients with both PNETs and RCC metastasis, in which it is difficult to determine the correct treatment tactics.

Differential diagnosis of PNETs and pancreatic RCC metastases by imaging methods is difficult due to the similarity of their imaging features. There are very few publications devoted to this problem. Kang et al. were among the first to reveal that the washout of the contrast agent in RCC metastases was significantly higher compared to PNETs in 16 patients with 37 RCC metastases and 28 patients with 31 PNETs [20]. With a washout threshold of 19% for RCC metastases, the accuracy, sensitivity, and specificity were 83.8%, 83.8%, and 83.9%, respectively. In our work, we could not evaluate the influence of contrast agent washout on the accuracy of diagnosing RCC metastases, since CT studies were performed at different institutions with different delay times, which could affect the results of the study. Lu et al. assessed the possibilities of a chemical shift artifact on the dual-echo gradient MRI in differentiation of RCC metastasis from PNETs [21]. The use of double echo made it possible to detect RCC metastases with sensitivity and specificity of 79.2% and 90.9%. However, the results obtained are limited to using the single institution standard protocol on a single MRI-machine. The use of the published algorithm in other centers and the reproducibility of the results were not evaluated during the work.

At the time of our study, two articles have been published on the use of texture analysis in the differential diagnosis of PNETs and RCC metastases to pancreas. Ambrosetti et al. assessed the performance of first-order texture features (histogram characteristics) using a two-dimensional region of interest on 29 RCC metastases and 27 PNETs [22]. In their work, only the Skewness (skewness of the histogram) was significantly different between the two types of neoplasms. However, it could not be used as a reliable differential diagnosis tool. Such negative results can be explained by the use of a two-dimensional region of interest and only first-order texture features, which significantly reduces the amount of information obtained from medical images. At the same time, van der Pol et al. on groups of 43 morphologically verified PNETs and 28 RCC metastases, revealed that the entropy has moderate sensitivity and specificity in the differential diagnosis of PNETs (71.4/79.1%, respectively), which allows it to be used for accurate differential diagnosis, but it is necessary further study on larger patient samples [17]. However, in contrast to our work, van der Pol et al. used only a two-dimensional region of interest and only first-order texture features, which could reduce the accuracy of texture analysis. Among the characteristics of contrast enhancement, their work evaluated only the homogeneity of the accumulation of the contrast agent, which, in our opinion, is very subjective, while the difference in the density of lesions and intact pancreatic parenchyma was not studied. At the same time, as in our work, van der Pol et al. did not reveal calcifications in the structure of RCC metastases.

Conclusion

Our diagnostic model is the first in the world to use a combination of contrast enhancement and texture features in the differential diagnosis of PNETs and pancreatic RCC metastases. It has high sensitivity (95.8%) with moderate specificity (62%) in the diagnosis of RCC metastasis to pancreas, which allows it to be used in complex diagnostic cases to determine the patient's treatment tactics.

References

1. Ouzaid I., Capitanio U., Staehler M. et al. Surgical Metastasectomy in Renal Cell Carcinoma: A Systematic Review. *Eur. Urol. Oncol*. 2019; 2 (2): 141–149. https://doi.org/10.1016/J.EUO.2018.08.028
2. Padala S.A., Barsouk A., Thandra K.C. et al. Epidemiology of Renal Cell Carcinoma. *Wld J. Oncol*. 2020; 11 (3): 79–87. https://doi.org/10.14740/WJON1279
3. Shah M.H., Goldner W.S., Benson A.B. et al. Neuroendocrine and Adrenal Tumors, Version 2.2021, NCCN Clinical Practice Guidelines in Oncology. *J. Natl. Compr. Canc. Netw*. 2021; 19 (7): 839–867. https://doi.org/10.6004/JNCCN.2021.0032
4. Campbell S.C., Uzzo R.G., Karam J.A. et al. Renal Mass and Localized Renal Cancer: Evaluation, Management, and Follow-up: AUA Guideline: Part II. *J. Urol*. 2021; 206 (2): 209–218. https://doi.org/10.1097/JU.0000000000001912
5. Almeida R.R., Lo G.C., Patino M. et al. Advances in Pancreatic CT Imaging. *Am. J. Roentgenol*. 2018; 211 (1): 52–66. https://doi.org/10.2214/AJR.17.18665
6. Lee N.J., Hruban R.H., Fishman E.K. Pancreatic neuroendocrine tumor: review of heterogeneous spectrum of CT appearance. *Abdom. Radiol*. 2018; 43 (11): 3025–3034. https://doi.org/10.1007/s00261-018-1574-4
7. Sellner F. Observations on Solitary Versus Multiple Isolated Pancreatic Metastases of Renal Cell Carcinoma: Another Indication of a Seed and Soil Mechanism? *Cancers*. 2019; 11 (9): 1379. https://doi.org/10.3390/CANCERS11091379
8. Nogueira M., Dias S.C., Silva A.C. et al. Solitary pancreatic renal cell carcinoma metastasis. *Autopsy. Case Reports*. 2018; 8 (2): e2018023. https://doi.org/10.4322/ACR.2018.023
9. Akirov A., Larouche V., Alshehri S. et al. Treatment Options for Pancreatic Neuroendocrine Tumors. *Cancers*. 2019; 11 (6): 828. https://doi.org/10.3390/CANCERS11060828
10. Barthet M., Giovannini M., Lesavre N. et al. Endoscopic ultrasound-guided radiofrequency ablation for pancreatic neuroendocrine tumors and pancreatic cystic neoplasms: A prospective multicenter study. *Endoscopy.* 2019; 51 (9): 836–842. https://doi.org/10.1055/A-0824-7067/ID/ JR17031-18
11. Fazio N., Kulke M., Rosbrook B. et al. Updated Efficacy and Safety Outcomes for Patients with Well-Differentiated Pancreatic Neuroendocrine Tumors Treated with Sunitinib. *Target. Oncol*. 2021; 16 (1): 27–35. https://doi.org/10.1007/S11523-020-00784-0/FIGURES/4
12. Quhal F., Mori K., Bruchbacher A. et al. First-line Immunotherapy-based Combinations for Metastatic Renal Cell Carcinoma: A Systematic Review and Network Meta-analysis. *Eur. Urol. Oncol.* 2021; 4 (5): 755–765. https://doi.org/10.1016/J.EUO.2021.03.001
13. Powles T., Albiges L., Bex A. et al. ESMO Clinical Practice Guideline update on the use of immunotherapy in early stage and advanced renal cell carcinoma. *Ann. Oncol*. 2021; 32 (12): 1511–1519. https://doi.org/10.1016/J.ANNONC.2021.09.014
14. Gu D., Hu Y., Ding H. et al. CT radiomics may predict the grade of pancreatic neuroendocrine tumors: a multicenter study. *Eur. Radiol*. 2019; 29 (12): 6880–6890. https://doi.org/10.1007/s00330-019-06176-x
15. Lin X., Xu L., Wu A. et al. Differentiation of intrapancreatic accessory spleen from small hypervascular neuroendocrine tumor of the pancreas: textural analysis on contrast-enhanced computed tomography. *Acta Radiol*. 60 (2019) 553–560. https://doi.org/10.1177/0284185118788895
16. Karmazanovsky G., Gruzdev I., Tikhonova V. et al. Computed tomography-based radiomics approach in pancreatic tumors characterization. *Radiol. Medica*. 2021; 126: 1388–1395. https://doi.org/10.1007/S11547-021-01405-0/FIGURES/1
17. van der Pol C.B., Lee S., Tsai S. et al. Differentiation of pancreatic neuroendocrine tumors from pancreas renal cell carcinoma metastases on CT using qualitative and quantitative features. *Abdom. Radiol*. 2019; 44(3): 992–999. https://doi.org/10.1007/s00261-018-01889-x
18. Nioche C., Orlhac F., Boughdad S. et al. Lifex: A freeware for radiomic feature calculation in multimodality imaging to accelerate advances in the characterization of tumor heterogeneity. *Cancer Res*. 2018; 78 (16): 4786–4789. https://doi.org/10.1158/0008-5472.CAN-18-0125
19. Gruzdev I.S., Zamyatina K.A., Tikhonova V.S. et al. Reproducibility of CT texture features of pancreatic neuroendocrine neoplasms. *Eur. J. Radiol*. 2020; 133: 109371. https://doi.org/10.1016/j.ejrad.2020.109371
20. Kang T.W., Kim S.H., Lee J. et al. Differentiation between pancreatic metastases from renal cell carcinoma and hypervascular neuroendocrine tumour: Use of relative percentage washout value and its clinical implication. *Eur. J. Radiol*. 2015; 84 (11): 2089–2096. https://doi.org/10.1016/J.EJRAD.2015.08.007
21. Lyu H.-L., Cao J.-X., Wang H.-Y. et al. Differentiation between pancreatic metastases from clear cell renal cell carcinoma and pancreatic neuroendocrine tumor using double-echo chemical shift imaging. *Abdom. Radiol*. 2018; 43 (10): 2712–2720. https://doi.org/10.1007/s00261-018-1539-7
22. Ambrosetti M.C., Zamboni G.A., Fighera A., Mansueto G. Pancreatic metastases from renal neoplasms and neuroendocrine pancreatic tumours: is a differential diagnosis possible with CT? *Hell. J. of Radiol.* 2019; 4 (3). 17–21. https://doi.org/10.36162/HJR.V4I3.295

Contact*: Ivan S. Gruzdev – 27, Bolshaya Serpukhovskaya str., Moscow 117997, Russian Federation. A.V. Vishnevsky National Medical Research Centre of Surgery. Phone: +7-903-517-93-20. E-mail address: gruzdev_van@mail.ru

Ivan S. Gruzdev – postgraduate student, Radiology department, A.V. Vishnevsky National Medical Research Center of Surgery, Moscow. https://orcid.org/0000-0003-0781-9898

Grigory G. Karmazanovsky – Academician of the Russian Academy of Sciences, doct. of med. sci., Professor of radiology department, Radiology department, A.V. Vishnevsky National Medical Research Center of Surgery, Moscow. https://orcid.org/0000-0002-9357-0998

Mariya G. Lapteva – PhD, radiologist, Radiology Department, N.N. Blokhin National Medical Research Center of Oncology, Moscow. https://orcid.org/0000-0003-2412-1299

Kseniia A. Zamiatina – postgraduate student, Radiology Department, A.V. Vishnevsky National Medical Research Center of Surgery, Moscow. https://orcid.org/0000-0002-1643-6613

Valeriya S. Tikhonova – postgraduate student, Radiology Department, A.V. Vishnevsky National Medical Research Center of Surgery, Moscow. https://orcid.org/0000-0001-9782-7335

Evgeny V. Kondratyev – PhD, senior researcher, Radiology Department, A.V. Vishnevsky National Medical Research Center of Surgery, Moscow. https://orcid.org/0000-0001-7070-3391

Vladimir Yu. Struchkov – PhD, junior researcher, Abdominal Surgery Department, A.V. Vishnevsky National Medical Research Center of Surgery, Moscow. https://orcid.org/0000-0003-1555-1596

Andrey V. Glotov – PhD, pathologist, Pathological Department, A.V. Vishnevsky National Medical Research Center of Surgery, Moscow. https://orcid.org/0000-0002-6904-9318

Ilya S. Proskuryakov – PhD, oncologist, Department of Interventional Radiology, N.N. Blokhin National Medical Research Center of Oncology, Moscow. https://orcid.org/0000-0002-4863-0832

Danil V. Podluzhnyi – PhD, Head of the Oncology Department of Surgical Treatment Methods (Hepato-pancreatobiliary Tumors), N.N. Blokhin National Medical Research Center of Oncology, Moscow. https://orcid.org/0000-0001-7375-3378.

Amiran Sh. Revishvili – Academician of the Russian Academy of Sciences, Doct. of Sci. (Med.), Professor, Director of A.V. Vishnevsky National Medical Research Center of Surgery, Moscow. https://orcid.org/0000-0003-1791-9163

Для корреспонденции*: Груздев Иван Сергеевич – 117997 Москва, ул. Большая Серпуховская, д 27. ФГБУ “НМИЦ хирургии

Груздев Иван Сергеевич – аспирант отделения рентгенологии и магнитно-резонансных исследований с кабинетом ультразвуковой диагностики, ФГБУ “НМИЦ хирургии им. А.В. Вишневского” Минздрава России, Москва. https://orcid.org/0000-0003-0781-9898

Кармазановский Григорий Григорьевич – академик РАН, доктор мед. наук, профессор, заведующий отделением рентгенологии и магнитно-резонансных исследований с кабинетом ультразвуковой диагностики ФГБУ “НМИЦ хирургии им. А.В. Вишневского” Минздрава России, Москва. https://orcid.org/0000-0002-9357-0998

Лаптева Мария Григорьевна – канд. мед. наук, врач рентгенолог отделения лучевой диагностики. ФГБУ “НМИЦ онкологии им. Н.Н. Блохина” Минздрава России, Москва. https://orcid.org/0000-0003-2412-1299

Замятина Ксения Андреевна – аспирант отделения рентгенологии и магнитно-резонансных исследований с кабинетом ультразвуковой диагностики, ФГБУ “НМИЦ хирургии им. А.В. Вишневского” Минздрава России, Москва. ORCID 0000-0002-1643-6613.

Тихонова Валерия Сергеевна – аспирант отделения рентгенологии и магнитно-резонансных исследований с кабинетом ультразвуковой диагностики, ФГБУ “НМИЦ хирургии им. А.В. Вишневского” Минздрава России, Москва. ORCID 0000-0001-9782-7335.

Кондратьев Евгений Валерьевич – канд. мед. наук, старший научный сотрудник отделения рентгенологии и магнитно-резонансных исследований с кабинетом ультразвуковой диагностики ФГБУ “НМИЦ хирургии им. А.В. Вишневского” Минздрава России, Москва. ORCID 0000-0001-7070-3391.

Стручков Владимир Юрьевич – канд. мед. наук, младший научный сотрудник отделения абдоминальной хирургии ФГБУ “НМИЦ хирургии им. А.В. Вишневского” Минздрава России, Москва. https://orcid.org/0000-0003-1555-1596

Глотов Андрей Вячеславович – канд. мед. наук, врач-патологоанатом Патолого-анатомического отделения ФГБУ “НМИЦ хирургии им. А.В. Вишневского” Минздрава России, Москва. https://orcid.org/0000-0002-6904-9318

Проскуряков Илья Сергеевич – канд. мед. наук, врач-онколог отделения интервенционной радиологии, ФГБУ “НМИЦ хирургии им. А.В. Вишневского” Минздрава России, Москва. https://orcid.org/0000-0002-4863-0832

Подулжный Данил Викторович – канд. мед. наук, заведующий хирургическим отделением №7 (опухолей гепатопанкреатобилиарной зоны) ФГБУ “НМИЦ онкологии им. Н.Н. Блохина” Минздрава России, Москва. https://orcid.org/0000-0001-7375-3378.

Ревишвили Амиран Шотаевич – академик РАН, доктор мед. наук, профессор, директор ФГБУ “НМИЦ хирургии им. А.В. Вишневского” Минздрава России, Москва. https://orcid.org/0000-0003-1791-9163